



CoA Note 125

R 24507/B

Second Rocket Propulsion Symposium

Cranfield.

April, 1962

'HEAT TRANSFER AT LOW TEMPERATURE IN THE ENTRY
SECTION OF A SOLID PROPELLANT ROCKET NOZZLE'

by

A.G. Smith, T.A. Carberry and R.M. Houston



R 24507/B

HEAT TRANSFER AT LOW TEMPERATURE IN THE ENTRY
SECTION OF A SOLID PROPELLANT ROCKET NOZZLE

by

A.G. Smith¹, T.A. Carberry² and R.M. Houston³.

SUMMARY

Heat transfer in the converging section of the nozzle of a simulated solid propellant rocket with a star-shaped conduit has been investigated in the following way:

- (a) Area-average heat transfer has been measured on a room-temperature rig, with and without a simulated charge.
- (b) Theoretical heat transfer has been calculated without the charge (axisymmetric laminar flow).
- (c) An attempt has been made to predict the detailed distribution of heat transfer by measurements of mass transfer on a nozzle made of naphthalene.
- (d) Flow visualisation has been performed on a water-rig.

Roughly, results are as follows, $5 \times 10^4 < R_D < 6 \times 10^5$:

(a) and (b):

With conduit, $Nu = 0.2 R_D^{0.63} Pr^{\frac{1}{3}}$, (Nu and R_D based on throat diameter and velocity).

Without conduit (corresponding to all-burnt)
 $Nu = 0.70 R_D^{0.49} Pr^{\frac{1}{3}}$, about 30% > theoretical, and about 50% < with conduit.

(c) and (d):

Marked circumferential variation of heat transfer occurred, related to a system of horse-shoe vortices, when the conduit was present. Contrary to expectations, heat transfer at the throat was not very different from elsewhere.

-
- 1. University of Nottingham.
 - 2. Department of Aircraft Propulsion,
The College of Aeronautics.
 - 3. Royal Canadian Navy.

Notation

C_p	specific heat at constant pressure
D	diameter of nozzle throat
h	coefficient of heat transfer, based on the difference between nozzle wall and stagnation temperature.
k	thermal conductivity of air, at stagnation temperature
Nu	Nusselt number, hD/k
Pr	Prandtl number, $\mu C_p/k$
R_D	Reynolds number, $\rho_t V_t D/\mu$
V_t	velocity of air, at the throat of the nozzle
ρ_t	density of air, at the throat of the nozzle
μ	viscosity of air, at stagnation conditions.

1.0 Introduction

Erosion phenomena have been noticed in the inlet section of solid propellant rocket motor nozzles, and part of the background necessary to understand these phenomena lies in the field of heat transfer.

Ideally a knowledge of heat transfer under the physical and chemical conditions of the actual rocket is required, but such knowledge is hard to obtain. It was felt however that it would be worthwhile to obtain knowledge of heat transfer on an air-rig, simulating a solid rocket in shape, but not in gas properties and temperature. Accordingly a small model rocket was constructed having a 4.5" diameter case and a charge was simulated by means of a perspex model. The flow conditions in the converging section of the nozzle were then investigated.

It is very difficult to measure heat transfer contours on a surface. Usually the most that is attempted, for axisymmetric shapes, is the variation axially of the mean circumferential heat transfer. One detailed technique is available however: that of measuring rate of mass transfer from a sublimating solid. Ref.(1). The technique is not easy: The sublimation rates are so small, that refined methods of measurement of the thickness of the layer of sublimed solid must be used. The rate of sublimation varies rapidly with temperature, so that the temperature of the solid must be accurately known. Vapour pressures of the available solids are not known as accurately as would be desired, and a delicate conversion from mass-transfer rates to heat-transfer rates must be made.

The way round these difficulties was apparently to check the mean heat transfer rates predicted from the mass transfer experiments by a separate heat transfer experiment. Then if agreement was obtained, well and good. If not, then it could be argued that at least the relative distribution of heat transfer derived from the mass transfer experiments would be reliable.

Distribution of heat transfer over the nozzle entry section is useful to know: but to facilitate the use of this knowledge in the design of more favourable geometries, the flow phenomena underlying the heat transfer distribution must be determined. The designer is then in a better position to speculate as to the effect of geometry changes on heat transfer. Flow visualisation on a water-model was therefore undertaken.

Finally a theoretical calculation of heat transfer in the entry section of the nozzle was made, under the assumption of laminar flow, to get an idea of whether relatively simple theory would give satisfactory answers.

2.0 Heat transfer measurements

Air was sucked through a conduit (7-point star) followed by a water-heated copper nozzle entry section (Fig. 1). Heat transfer rates were obtained by measurements of air mass flow and the temperature drop of the heating water. Refined techniques were used to secure repeatability and absolute accuracy of results. Time-variations of water inlet temperature, (which would result in thermal inertia effects) were eliminated by use of a very sensitive 'drift indicator' in the hot water line. Water temperature drop (about 30°) was measured by a calibrated thermocouple and checked by mercury-in-glass thermometers. Water flow rate was measured by a flowmeter calibrated by weighing. Tare heat leakage was measured at zero airflow, with the nozzle stuffed with cottonwool. The tare was about 5% of the total heat transfer. The whole rig is shown in Fig. 2.

Results are shown in Fig. 3, graphs A and B.

Points to note are:

- (a) A satisfactory line through the experimental values is (with charge present)

$$Nu = 0.20 R_D^{0.63} Pr^{\frac{1}{3}}. \quad [Nu, R_D, \text{ based on nozzle throat diameter and throat velocity and temperature}].$$

- (b) Two distances of the charge from the nozzle end were used: 0" and $\frac{3}{4}$ ". No significant change in the heat transfer coefficient was found.

- (c) There is fair agreement between measured heat transfer and the curve for turbulent pipe-flow (curve c). While this agreement is fortuitous, it serves to provide a reference for the magnitude of the results.

- (d) Reynolds and Mach No. varied simultaneously and their effects cannot be disentangled. The throat Mach number was unity at the highest Reynolds number.

- (e) Without the charge (corresponding to all-burnt, or to a cigarette-burning charge) the experimental heat transfer is given by:

$$Nu = 0.70 R_D^{0.49} Pr^{\frac{1}{3}}$$

This is some 40% lower than the Nusselt number with the charge present.

- (f) Most points lie within $\pm 4\%$ of the mean line drawn through them.



2.1 Heat transfer calculations

These were made by the method of Smith and Spalding (Ref. 3) for axisymmetric laminar flow, using velocity distributions determined experimentally. The theoretical curve is shown as line D in Fig. 3. It is 25% below the experimental value. The discrepancy is not understood.

3.0 Mass transfer experiments

The basic idea is that a vapour diffuses into an air stream like heat. Concentration gradient drives mass via a diffusion coefficient in the same way that temperature gradient drives heat via the thermal conductivity. So if the rate of convection of vapour from a surface can be measured for a known concentration difference between surface and mainstream, it should be possible to compute the rate of convection of heat from this surface for a given difference of temperature between surface and mainstream, provided of course, that the Schmidt number for the mass transfer is equal to the Prandtl number for the heat transfer.

The vapour was provided by making a nozzle of naphthalene, whose vapour pressure is known as a function of temperature. Air was sucked through the nozzle with the same airflow arrangements as for the heat transfer measurements (Fig. 2). The naphthalene surface profile was measured before and after convection, on a 'Talyrond' machine. 'Reference strips' were painted on the naphthalene surface to prevent evaporation locally and thus to provide a 'post convection datum'. A detailed description of the technique is given in Ref. 2. Typical measurements as shown on Fig. 4 indicate a fairly large variation of mass transfer rate over the surface.

Mean Nusselt numbers (heat) deduced from the mass transfer measurements are shown as curve E on Fig. 3. The discrepancy with the heat transfer measurements is probably due to errors in the naphthalene diffusion coefficient and vapour pressure data which were used.

Ratios of max-to-mean deduced heat transfer coefficients are given in Table 1. The main weakness in the experiment lies, probably, in uncertainty as to Naphthalene surface temperature. At the lowest Reynolds numbers, where Mach numbers were low too, the estimates of surface temperature were probably satisfactory. As Mach numbers approached unity, errors in the assumed recovery factor would be important.

TABLE 1

$10^{-5} \times R_D$	7.0	6.7	5.2	4.0	3.3	2.4	2.1	1.7	1.4	0.9
$h \text{ max.}/\bar{h}$	1.5	1.6	1.5	1.5	1.5	1.6	1.6	1.5	1.6	1.75
Annulus	B	C	C	C	C	B	B	B	B	B
at which	and						and	and		and
this occurs	C						C	C		C

4.0 Flow visualisation

The water flow visualisation apparatus is shown in Fig.5. The water-filled glass tank (top left) contains the nozzle and conduit model. Water with 0.03" polystyrene pellets was pumped through it and viewed with a plane beam of light about 0.1" thick. Photographs as illustrated in Fig.6 were obtained. From these and careful observations of the rig, a flow diagram (Fig.7) was concocted. Prolonged study of this will reveal

- 1) a 'horseshoe' vortex in the wake of each solid-star point.
- 2) a 'petal' vortex near the nozzle surface, displaced one half star pitch from the horseshoe vortex.

These vortices correspond to a reverse-flow region in the wake of the solid star-point.

As might be expected, the impingement of the gas-star point on the nozzle corresponds to a point of high mass transfer. An unexpected result, however is the 'pip' of high mass transfer in between the expected high points. This 'pip' appears to be associated with the confluence of the 'splash' from the gas-star impingement regions.

Discussion

The work reported here adds appreciably to knowledge about heat transfer in rocket nozzles. There are quite a few gaps in the work, such as unexplained discrepancies between heat and mass transfer measurements and the laminar-flow theory, and the essential combination of Reynolds and Mach Number effects. To fill up these gaps would demand

- a) Heat transfer measurements on a variable-density rig.
- b) Further work on a naphthalene model combined with calibration of the method by experiments on laminar flow cases which can be accurately calculated.

Perhaps the main points emerging are:

- (a) If Mach Number effects are small, (which the authors think probable) the $Nu \sim R_D$ relation will be a true one, and might possibly be extrapolated upwards in R_D by a factor of 2 or 3.
- (b) The mass-transfer measurements indicate the probability of max/mean heat transfer coefficients of the order of 1.6.
- (c) There will be a substantial decrease in heat transfer coefficient between starting and all-burnt.
- (d) Laminar-flow theory fails to predict heat transfer coefficients accurately over the R_D range tested (without charge).
- (e) The distance between the charge and the nozzle does not affect the heat transfer coefficient, at least over the range of distance tested.

References

- 1. Grober, Erk, and Grigull 'Fundamentals of Heat Transfer'. McGraw-Hill 1961.
- 2. Houston, R.M. 'Nozzle heat transfer prediction from sublimation measurements on a model of a solid fuel rocket'. College of Aeronautics Thesis, June 1960.
- 3. Smith, A.G. and Spalding, D.B. 'Heat transfer in a laminar boundary layer with constant fluid properties and constant wall temperature'. J. Roy. Aero. Soc. 62. 60 (1958)



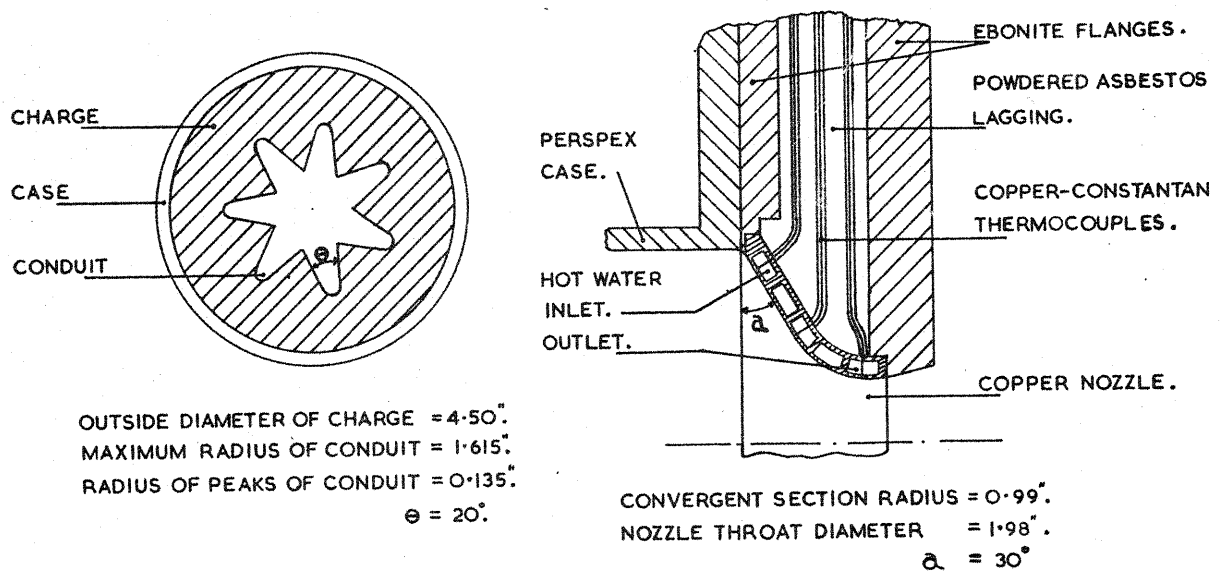


FIG.1. CROSS-SECTION OF CHARGE & COPPER NOZZLE.

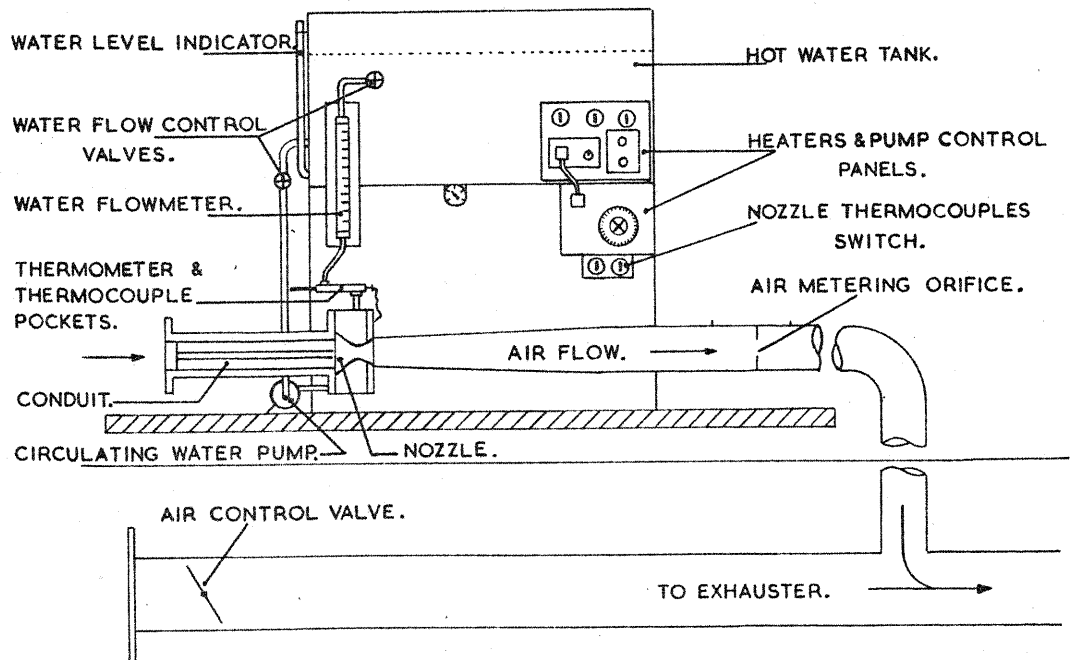
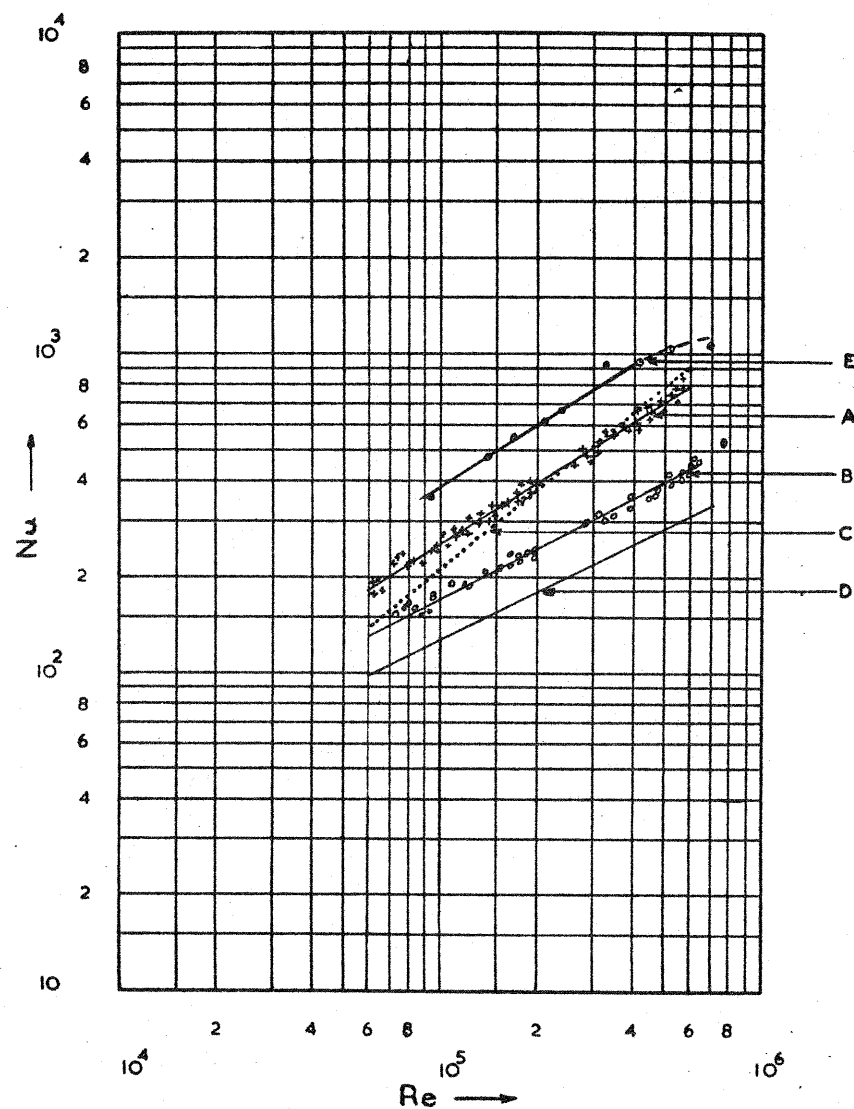


FIG.2. DIAGRAMMATIC LAYOUT OF HEAT TRANSFER RIG.



A & B. HEAT TRANSFER RESULTS.

A. CHARGE BEFORE NOZZLE. "

$$Nu = 0.20 \cdot Re_B^{0.63} \cdot Pr^{1/3}$$

B. CHARGE REMOVED.

$$Nu = 0.70 \cdot Re_D^{0.49} \cdot Pr^{1/3}$$

C. $Nu = 0.023 \cdot Re^{0.8} \cdot Pr^{0.4}$

FOR FULLY DEVELOPED

TURBULENT FLOW IN PIPES.

D. $Nu = 0.395 \cdot Re^{0.5}$ FOR $Pr = 0.7$.

THEORETICAL RESULT FOR
AXISYMMETRIC LAMINAR FLOW.

E. MASS TRANSFER RESULTS
CHARGE BEFORE NOZZLE.

FIG. 3. EXPERIMENTAL RESULTS.

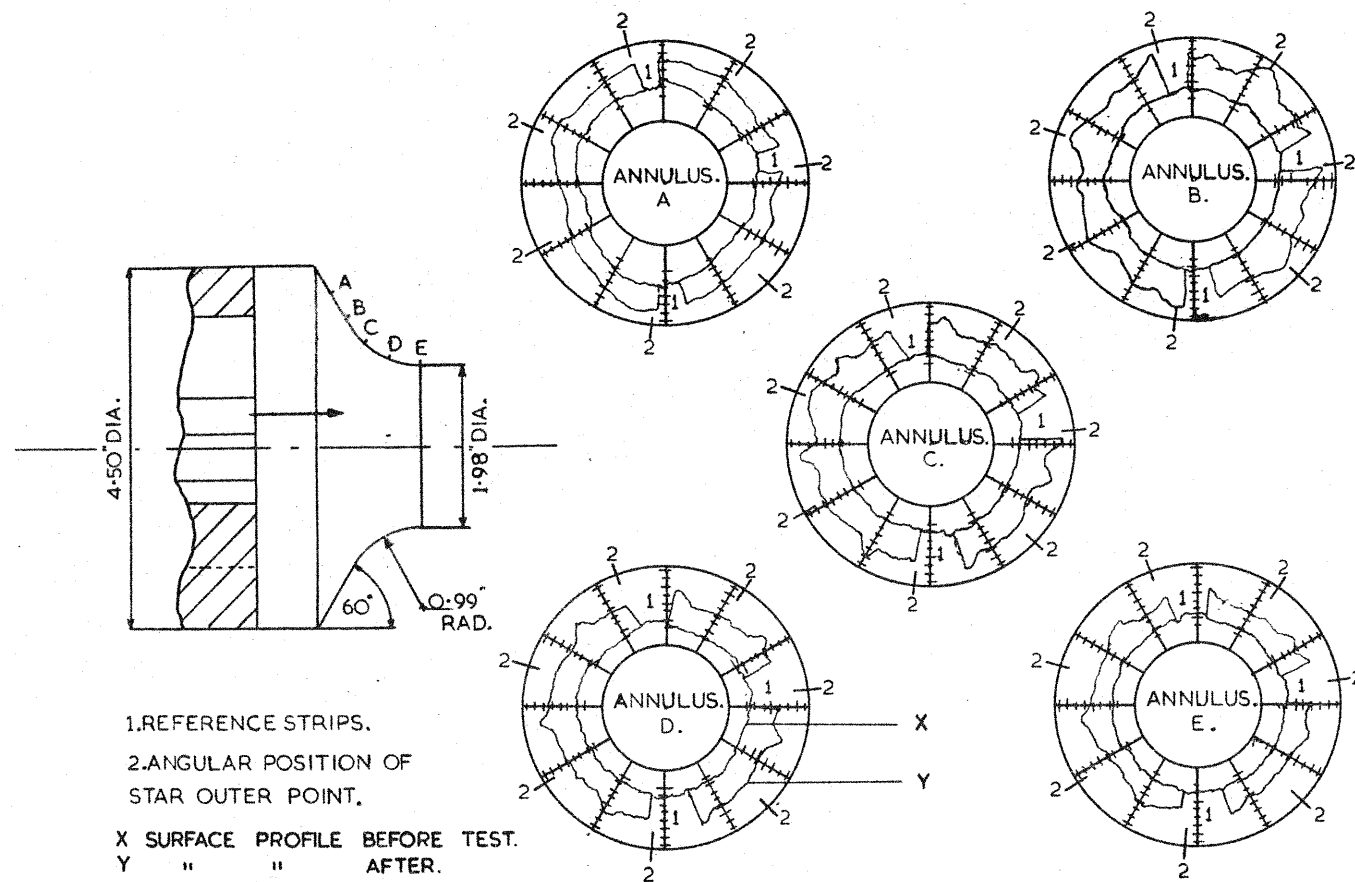


FIG. 4. TYPICAL "TALYROND" MEASUREMENTS FROM MASS TRANSFER EXPERIMENTS.

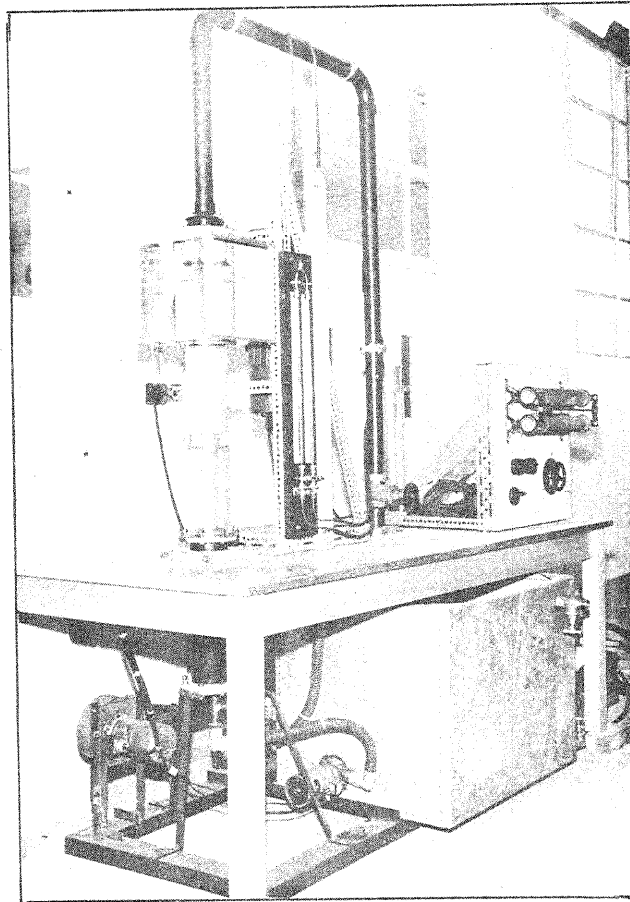


FIG. 5. FLOW VISUALISATION APPARATUS

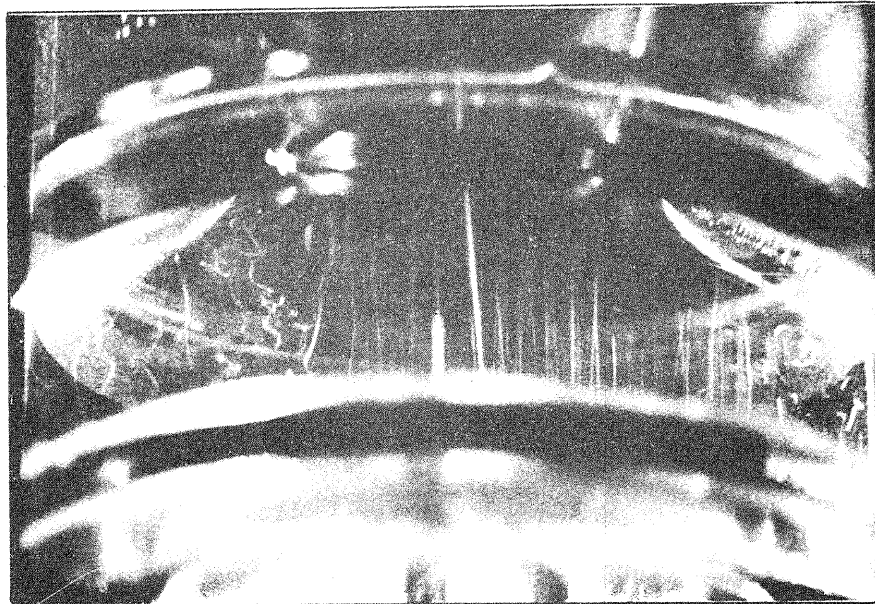
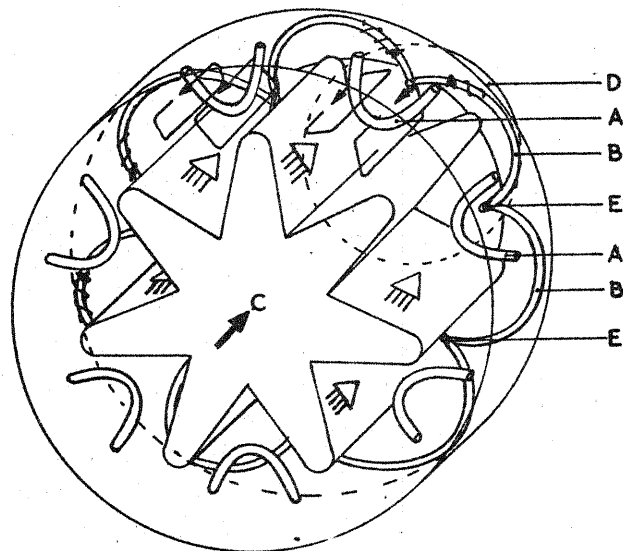


FIG. 6. FLOW VISUALISATION PHOTOGRAPH



- VORTEX CORE.
- FLOW DIRECTION.
- A. "HORSE-SHOE" VORTEX.
- B. "PETAL" VORTEX.
- C. MAIN FLOW LEAVING CONDUIT.
- D. NOZZLE (CONVERGENT SECTION ONLY)
- E. TURBULENT MIXING OF "PETAL" VORTICES.

FIG. 7. FLOW PATTERN REPRESENTATION.